Development 134, 4335-4345 (2007) doi:10.1242/dev.012047

Blimp1 regulates development of the posterior forelimb, caudal pharyngeal arches, heart and sensory vibrissae in mice

Elizabeth J. Robertson[1,*], Iphigenie Charatsi[1], Clive J. Joyner[1], Chad H. Koonce[1], Marc Morgan[1], Ayesha Islam[1], Carol Paterson[1], Emily Lejsek[1], Sebastian J. Arnold[1], Axel Kallies[2], Stephen L. Nutt[2] and Elizabeth K. Bikoff[1,*]

The zinc-finger transcriptional repressor Blimp1 (Prdm1) controls gene expression patterns during differentiation of B lymphocytes and regulates epigenetic changes required for specification of primordial germ cells. *Blimp1* is dynamically expressed at diverse tissue sites in the developing mouse embryo, but its functional role remains unknown because *Blimp1* mutant embryos arrest at E10.5 due to placental insufficiency. To explore *Blimp1* activities at later stages in the embryo proper, here we used a conditional inactivation strategy. A *Blimp1-Cre* transgenic strain was also exploited to generate a fate map of *Blimp1*-expressing cells. *Blimp1* plays essential roles in multipotent progenitor cell populations in the posterior forelimb, caudal pharyngeal arches, secondary heart field and sensory vibrissae and maintains key signalling centres at these diverse tissues sites. Interestingly, embryos carrying a hypomorphic $Blimp1^{gfp}$ reporter allele survive to late gestation and exhibit similar, but less severe developmental abnormalities, whereas transheterozygous $Blimp1^{gfp/-}$ embryos with further reduced expression levels, display exacerbated defects. Collectively, the present experiments demonstrate that *Blimp1* requirements in diverse cell types are exquisitely dose dependent.

KEY WORDS: *Blimp1* (*Prdm1*), Forelimb, ZPA, Shh, Fgf8, Tbx1, Pharyngeal epithelium, Heart morphogenesis, Sensory vibrissae

INTRODUCTION

The zinc-finger transcriptional repressor, Blimp1 (also known as Prdm1), originally identified as a silencer of β-interferon gene expression (Keller and Maniatis, 1991) and a master regulator controlling terminal differentiation of B lymphocytes (Turner et al., 1994), also governs T-lymphocyte homeostasis (Kallies et al., 2006; Martins et al., 2006), primordial germ cell (PGC) specification (Ohinata et al., 2005; Vincent et al., 2005) and stem cell maintenance in the sebaceous gland (Horsley et al., 2006). *Blimp1* functions to regulate cell cycle progression and globally redirects patterns of gene expression (Shaffer et al., 2002; Ohinata et al., 2005; Shapiro-Shelef and Calame, 2005; Kallies and Nutt, 2007). Blimp1 contains an N-terminal PR/SET domain, a proline-rich region, five C_2H_2 zinc fingers and a C-terminal acidic domain (Tunyaplin et al., 2000; Turner et al., 1994). The zinc-finger region mediates nuclear import and DNA binding (Keller and Maniatis, 1992; Gyory et al., 2003; Gyory et al., 2004). The evolutionarily conserved PR/SET domain, closely related to histone methyl transferases, recruits additional epigenetic modifiers that cooperatively function to modify chromatin structure and mediate gene silencing (Ren et al., 1999; Yu et al., 2000; Gyory et al., 2004; Ancelin et al., 2006; Hayashi et al., 2007; Surani et al., 2007). Recent experiments suggest that the transcriptional networks controlled by *Blimp1* are cell-type specific. For example, Blimp1 represses *c-myc* (also known as *Myc* – Mouse Genome Informatics) expression in mature B cells (Lin et al., 1997) and sebaceous gland progenitors (Horsley et al., 2006) but *c-myc* is not a transcriptional target in activated T-effector cells (Gong and Malek, 2007). In addition to governing exit from the cell cycle, Blimp1 also protects plasma cells from ER stress by maintaining XBP expression, a key transcription factor required for immunoglobulin secretion (Shaffer et al., 2004). Blimp1 has impressive abilities to regulate cell growth, differentiation and survival through its diverse molecular partnerships in highly specialised cell types.

Blimp1-deficient embryos die around embryonic day (E) 10.5 (Vincent et al., 2005) because of widespread haemorrhaging and blood pooling within the dorsal aortae. The primitive heart seems to function normally, but placental development is severely compromised. *Blimp1* mutants fail to expand the labyrinthine region where the bulk of foetal and maternal exchange takes place leading to placental insufficiency. In the embryo proper *Blimp1* is strongly expressed in the key signalling centres that pattern the forebrain, namely the leading anterior mesendoderm and prechordal plate, but development of the head structures proceeds normally in *Blimp1* mutants. Strikingly *Blimp1* functional loss disrupts PCG specification (Ohinata et al., 2005; Vincent et al., 2005). *Blimp1* silences the default somatic pathway and allows a few epiblast cells to become exclusively allocated into the germ cell lineage (reviewed by Hayashi et al., 2007). At later stages, *Blimp1* is transiently expressed in subsets of the pharyngeal endoderm and ectoderm, splanchnic mesoderm, endothelial cells and somites (Vincent et al., 2005), and in the papillae of the teeth, hair and taste buds (Chang et al., 2002). Owing to the early lethality, possible *Blimp1* functions in these diverse tissues have yet to be elucidated.

To bypass placental defects and examine *Blimp1* activities in the embryo, here we used a *Sox2-Cre* deleter strain (Hayashi et al., 2002) in conjunction with a *Blimp1* conditional allele (Shapiro-Shelef et al., 2003). *Blimp1* functions normally in the extra-embryonic cell lineages and as a result, mutant embryos survive to late gestation stages. The present experiments demonstrate that *Blimp1* is required for development of the posterior forelimb bud, pharyngeal epithelia, the secondary heart field (SHF) and dermal papillae (DP) of the sensory vibrissae. *Blimp1* maintains expression of key signalling molecules and coordinates cell proliferation and differentiation at these diverse tissue sites. Additionally we characterised *Blimp1* mutant embryos carrying an IRES-*gfp* reporter

[1]Sir William Dunn School of Pathology, University of Oxford, South Parks Road, Oxford OX1 3RE, UK. [2]The Walter and Eliza Hall Institute of Medical Research, Parkville, Victoria, 3050, Australia.

*Authors for correspondence (e-mails: Elizabeth.Robertson@path.ox.ac.uk; Elizabeth.Bikoff@path.ox.ac.uk)

Accepted 14 September 2007

allele that survive to late gestation (Kallies et al., 2004). In addition to expression of truncated Blimp1 protein lacking the C-terminal zinc fingers (Kallies et al., 2004), *Blimp1*$^{gfp/gfp}$ embryos also express full-length Blimp1 protein. These embryos display forelimb, pharyngeal and heart defects and a complete loss of germ cells, but sensory vibrissae develop normally. Interestingly, double heterozygotes carrying the hypomorphic *Blimp1*^{gfp} allele and a null allele display more severe defects that closely resemble those described here for *Blimp1* mutants. Collectively, the present experiments demonstrate that *Blimp1* requirements in diverse progenitor cell populations are exquisitely dose dependent.

MATERIALS AND METHODS

Mouse strains and genotyping procedures

The *Prdm1*^{BEH} (Vincent et al., 2005), *Prdm1*^{flox} (Shapiro-Shelef et al., 2003), *Blimp1*^{gfp} (Kallies et al., 2004) targeted alleles and R26R reporter mice (Soriano, 1999) have been described. Mice and embryos were genotyped by PCR as described in the original reports. The *Sox2-Cre* (Hayashi et al., 2002), *Tie2-Cre* (Kisanuki et al., 2001) and *Blimp1-Cre* (Ohinata et al., 2005) transgenic strains were maintained on a mixed outbred background and genotyped using Cre-specific PCR.

Whole-mount in situ hybridisation, *lacZ* staining and histology

Embryos were fixed overnight in 4% paraformaldehyde (PFA). Whole-mount in situ hybridisation on intact embryos was performed according to standard protocols. Standard probes specific for *Shh*, *Fgf8*, *Fgf4*, *Tbx2*, *Tbx3*, *Ptc1*, *Gli1*, *Lmx1*, *Tbx1*, *Blimp1*, *Bmp4*, *Grem1* and *Cre* were used. X-gal staining was performed as described (Nagy et al., 2003). Embryos were post fixed, photographed, dehydrated and embedded for histology. Sections (8 μm) were mounted and counterstained with eosin. For standard histology, material was fixed overnight in 4% PFA in PBS and processed for standard haematoxylin and eosin staining. Hearts were manually dissected, photographed and processed as above.

Immunohistochemistry

Embryos were fixed overnight in 4% PFA, dehydrated in ethanol, embedded and sectioned at 6 μm. Sections were subject to antigen retrieval by boiling for 20 minutes in either Antigen Retrieval Solution (DAKO), (Ki67 and phosphohistone 3 staining) or Tris-EDTA pH 9.0 (c-myc staining), blocked for 5 minutes in peroxidase block (DAKO K4011), washed in PBS, incubated in primary antibody overnight at 4°C, washed in PBS and developed using the appropriate DAKO peroxidase-labelled polymer kit and DAB, and counterstained with haematoxylin. Antibodies were anti-c-myc (Santa Cruz N-262, sc-764 1:250), Ki67 (NovoCastra NCL-L-MM1, 1:200) and anti-phosphohistone 3 (Upstate 06-570, 1:200). For visualisation of apoptotic cells, embryos were incubated for 30 minutes at 37°C in Lysotracker Red (Molecular Probes L-7528 RED; diluted 1:400 in Hank's balanced salt solution), washed in HBSS, fixed overnight in 4% PFA, dehydrated in methanol and viewed by fluorescence microscopy.

Alkaline phosphatase staining

PGCs were visualised at E9.5 by staining for alkaline phosphatase activity, flat mounted under coverslips in 80% glycerol, and photographed under bright-field microscopy as described previously (Lawson et al., 1999).

Skeleton preparations

Intact embryos or isolated limbs were fixed in Bouin's and cartilage and bone were stained using Alcian Blue and Alizarian Red as described (Nagy et al., 2003). Specimens were cleared in benzyl alcohol:benzyl benzoate (1:1) before photography.

RT-PCR analysis

Total RNA from STO fibroblasts, individually genotyped E9.5 mouse embryos, or spleen cells cultured with LPS was prepared using Trizol (Invitrogen). The OneStep RT-PCR kit (Qiagen) was used with *Blimp1* primer pairs (Exon 6 forward, 5′-CGGAAAGCAACCCAAAGCAATAC-3′ and Exon 6 reverse, 5′-CCTCGGAACCATAGGAAACATTC-3′; Exon 6 forward, 5′-GGTTACAAGACTCTTCCTTAC-3′ and Exon 8 reverse, 5′-GCTCTTGTGACACTGGGCACA-3′; Exon 8 forward, 5′-GCAATCTCAAGACCCACCTTC-3′ and Exon 8 reverse, 5′-CGAACCTCTCAATTTCTTCATT-3′), and *Hprt* primer pair (forward, 5′-GCTGGTGAAAAGGACCTCT-3′ and reverse, 5′-CACAGGACTAGAACACCTGC-3′) with an annealing temperature of 58°C for 30 cycles.

Western blots

Spleen cells cultured for 3 days in the presence of LPS (50 μg/ml), were washed and the cell pellets lysed in buffer containing 1% Nonidet P-40, 20 mM Tris-HCl (pH 7.5), 150 mM NaCl, 5 mM EDTA, and protease inhibitors (Sigma). Individually genotyped E9.5 embryos were lysed in RIPA buffer plus protease inhibitors (Sigma). Extracts were centrifuged for 30 minutes at 20,800 ***g***. Lysates were mixed with 2× Laemmli buffer and boiled for 5 minutes before fractionation on an 8% polyacrylamide gel. Proteins were transferred onto a nitrocellulose membrane (catalogue BA83; Schleicher & Schüll) for 2 hours at 500 mA. Membranes rinsed in TBS-T were blocked for 1 hour in TBS-T with 5% dried milk, and incubated at 4°C overnight with rat monoclonal anti-Blimp1 (Kallies et al., 2004) then secondary antibody (goat anti-rat Ig, cat. no. NA935; Amersham Biosciences) and developed by chemiluminescence using ECL Plus (Amersham Biosciences).

Immunofluorescence microscopy

Full-length *Blimp1* cDNA (Turner et al., 1994) and mutagenised *Blimp1* were subcloned into a modified version of pCAGGS (Niwa et al., 1991). For mutagenesis, Val556 of the *Blimp1* coding sequence was changed to a stop codon using the QuikChange II Site-Directed Mutagenesis Kit (Stratagene). Primers used for mutagenesis were 5′-GCTCTCCAACCTGAAGTAA-CACCTGAGAGTGCAC-3′ (sense) and 5′-GTGCACTCTCAGGTGT-TACTTCAGGTTGGAGAGC-3′ (antisense). COS cells were grown on coverslips and transfected with 0.8 μg DNA complexed with Lipofectamine 2000 (Invitrogen). Cells were washed with PBS, fixed with 4% formaldehyde, quenched with NH_4Cl, incubated in blocking buffer containing 2.5% goat serum, 2.5% donkey serum, 2% bovine serum albumin (BSA), 2% fish skin gelatin (Sigma) and 2.5% Triton X-100 and incubated overnight at 4°C in blocking buffer containing mouse monoclonal anti-Blimp-1 (1:200, Novus Biologicals). After three rinses, coverslips were incubated for 1 hour at room temperature in blocking buffer containing secondary antibody (1:2000 dilution, Invitrogen A11029), rinsed and placed inverted onto a drop of mounting medium containing DAPI (Vectashield, Vector Laboratories). Samples were visualised with a Zeiss LSM510 META confocal microscope.

RESULTS

Blimp1 expression in the extra-embryonic cell tissues rescues development

It seemed likely that *Blimp1* null embryos die by E10.5 due to placental defects, but loss of *Blimp1* expression in the developing endothelium (Vincent et al., 2005) might also compromise integrity of the blood vessels. To distinguish these possibilities, mice homozygous for the *Prdm1* conditional allele (Shapiro-Shelef et al., 2003) (*Prdm1*$^{flox/flox}$) were crossed to *Sox2-Cre* transgenic mice

Table 1. Functional *Blimp1* in the extra-embryonic lineages rescues development of the embryo proper

***Prdm1*$^{+/-}$ × *Prdm1*$^{+/-}$ Intercross**		
Age	Number of embryos	Recovery of *Prdm1*$^{-/-}$
E9.5	108	28 (25.9%)
E14.5	52	0 (0)
***Sox2-Cre;Prdm1*$^{BEH/+}$ × *Prdm1*$^{flox/flox}$ Intercross**		
Age	Number of embryos	Recovery of *Cre*$^{+}$*;Prdm1*$^{BEH/flox}$
E10.5	179	48 (26.8%)
E11.5	91	22 (24.2%)
E12.5	24	6 (25.0%)
E13.5	32	9 (28.0%)
E14.5	41	11 (26.8%)
E16.5	31	7 (22.5%)

(Hayashi et al., 2002) also carrying the *Prdm1*^{BEH} null allele (Vincent et al., 2005). *Sox2-Cre* activated at the blastocyst stage is exclusively expressed in epiblast derivatives: that is, only the embryo proper (Hayashi et al., 2002). *Sox2-Cre Prdm1*$^{BEH/flox}$ embryos were collected at E10.5 through to E16.5 (Table 1). As expected, homozygous *Prdm1*$^{-/-}$ or *Prdm1*$^{BEH/BEH}$ null embryos failed to survive beyond E10.5. By contrast, *Sox2-Cre Prdm1*$^{BEH/flox}$ embryos (hereafter referred to as *Blimp1* mutant embryos) were present at mendelian frequencies at E16.5 (Table 1), and were still viable at E18.5 (data not shown). However, we failed to recover live *Blimp1* mutants in newborn litters.

The rescued embryos displayed normal blood vessels. Additionally, conditional inactivation of *Blimp1* in endothelial cells using the well described *Tie2-Cre* transgene (Kisanuki et al., 2001) yielded viable animals. Mendelian numbers of *Tie2-Cre Prdm1*$^{BEH/flox}$-positive weanlings were recovered (22 out of 93), from crosses between *Tie2-Cre Prdm1*$^{BEH/+}$ and *Prdm1*$^{flox/flox}$ animals. We therefore conclude that the early lethality of *Blimp1* null embryos exclusively reflects *Blimp1* requirements in the extra-embryonic cell lineages and is not caused by endothelial cell defects.

At late gestational stages *Sox2-Cre*-rescued embryos consistently displayed two overt abnormalities. The forelimbs were missing posterior digits and sensory vibrissae were absent. Otherwise mutant embryos were indistinguishable from wild-type and heterozygous littermates. PCR genotyping of a large panel of individual mutant embryos confirmed that these overt defects were associated with efficient and complete Cre recombination (see Fig. S1 in the supplementary material).

Progenitors of the proximal posterior forelimb are selectively lost in *Blimp1* mutants

Blimp1 mRNA expression in the mesenchyme marks the developing forelimb and hindlimb buds coincident with their emergence (Vincent et al., 2005). During limb bud outgrowth *Blimp1* expression was restricted to the posterior mesenchyme encompassing the zone of polarising activity (ZPA) (Fig. 1). By E12.5 *Blimp1* expression in the mesenchyme was downregulated, and *Blimp1* transcripts were weakly induced in the apical ectodermal ridge (AER) (Fig. 1H, and data not shown). To further characterise forelimb defects, the elements of the appendicular

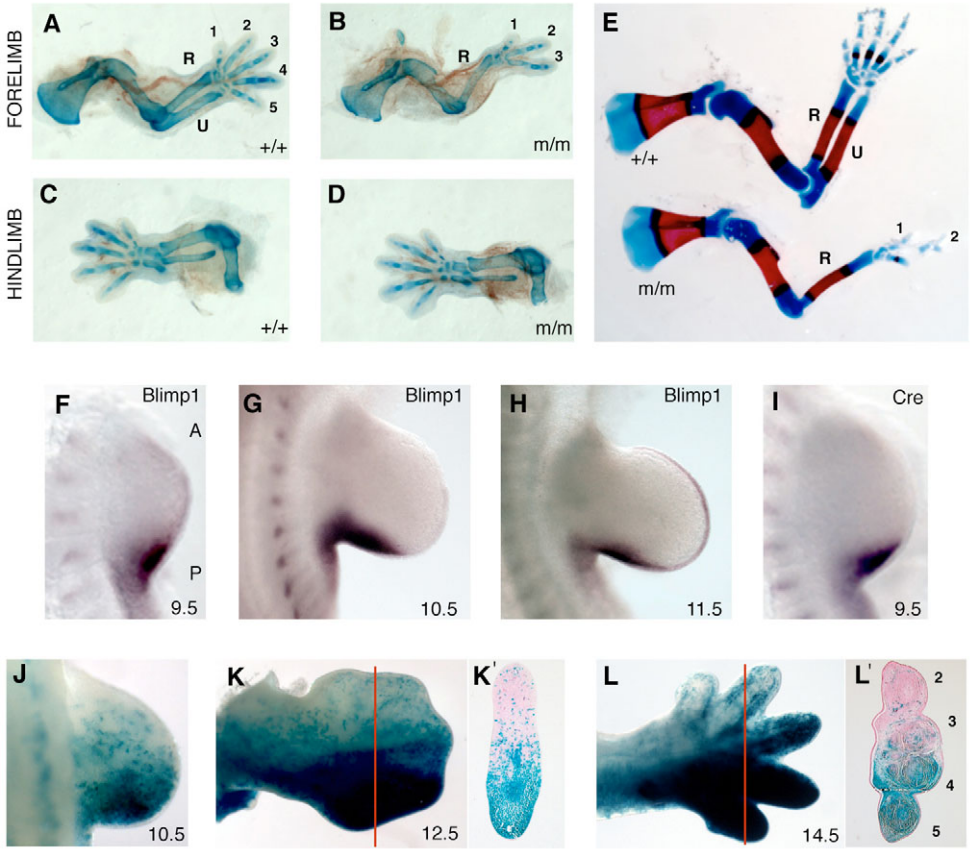

Fig. 1. Formation of the ulna and posterior forelimb digits requires *Blimp1* expression. (**A-D**) Alcian Blue staining of E13.5 control (+/+) and mutant (m/m) forelimbs (A,B) and hindlimbs (C,D) reveals absence of the ulna and fourth and fifth digits in *Blimp1* null-embryo forelimbs, whereas hindlimbs develop normally. (**E**) At E16.5, Alcian Blue-Alizarian Red staining shows that growth, patterning and ossification of the residual long bones and digits proceeds normally in the mutant. (**F-H**) Whole-mount in situ hybridisation (WISH) showing *Blimp1* expression is initially confined to the posterior mesoderm at E9.5 (F) and is rapidly downregulated over the next 48 hours (G,H). At E11.5, *Blimp1* expression is also detectable in the AER. (**I**) WISH shows that the *Blimp1-Cre* transgene faithfully recapitulates the pattern of endogenous *Blimp1* expression. Cell-fate mapping studies in the forelimb demonstrate that Blimp1+ cells initially confined to the posterior mesenchyme at E10.5 (**J**), give rise to the posterior half of the limb bud by E12.5 (**K**,**K'**). (**L**,**L'**) At E14.5, these mesodermal derivatives form the entire fourth and fifth posterior digits and the posterior half of the third digit, and the ulna. Blimp1^{+} cells also give rise to the posterior muscles, and connective tissues (L'). Diffuse staining in the dorsal limbs is due to the presence of *lacZ*-expressing endothelium. The fate map observed for Blimp1^{+} cells in the hindlimbs was identical. A, anterior; P, posterior; R, radius; U, ulna.

skeleton were visualised at E13.5 and 16.5 using Alcian Blue and Alizarian Red staining. As shown in Fig. 1A-E, the forelimbs attained normal size and the skeletal elements were correctly proportioned. However, the posterior proximal elements, and associated muscles and connective tissue were completely absent (see Fig. S2 in the supplementary material). Thus mutant forelimbs entirely lacked the ulna, and either two (7/15) or three (8/15) of the posterior digits, but were otherwise indistinguishable from the wild type.

The signalling centres controlling outgrowth and patterning of the early limb bud are well characterised (reviewed by Tickle, 2006; McGlinn and Tabin, 2006). Anterior-posterior (A-P) polarity is patterned by *Shh* signalling from the ZPA, proximal-distal (P-D) outgrowth is controlled by *Fgf* signalling from the AER, whereas the dorsal-ventral (D-V) axis requires *Wnt* signals from the dorsal ectoderm. The AER and ZPA are maintained by reciprocal inductive interactions between *Fgf* and *Shh* signalling pathways. We previously found at E9.5 that limb bud formation initiates normally, and *Shh* and *Fgf8*, markers of the ZPA and AER, respectively, are correctly induced in *Blimp1* mutant embryos (Vincent et al., 2005).

To further evaluate the forelimb patterning defects observed here, we analysed a panel of molecular markers between E10.5 and 12.5 (Fig. 2). *Shh* expression in the ZPA was induced with the appropriate temporal and spatial kinetics in both forelimbs and hindlimbs (Fig. 2A,B). However, *Shh*$^+$ ZPA progenitor cells in the forelimb are short-lived. Thus *Shh* transcripts are prematurely downregulated, and except for a small patch of expression corresponding to the distal-most edge of the ZPA (Fig. 2C,D), are largely absent by E11.5. Analysis of *Fgf* expression (Fig. 2G-J; see Fig. S3 in the supplementary material), together with the observation that mutant forelimbs attain wild-type length, demonstrated that the AER is correctly induced and at early stages seems to function normally. However, premature cessation of *Shh* signalling resulted in a failure to maintain localised *Fgf8* expression within the AER and as a result, the posterior region of the AER was selectively lost (Fig. 2J; see Fig. S3 in the supplementary material). Nonetheless, digit 2, which depends on paracrine *Shh* signalling (Harfe et al., 2004), was correctly patterned (Fig. 1). The *Shh* target genes *Ptch1* and *Gli1* were activated (Fig. 2P, data not shown). Thus the ZPA functions appropriately to impart initial A-P pattern. However, at later stages, *Blimp1* mutant forelimbs displayed truncated expression of posterior markers genes, such as *Tbx2* (Fig. 2M,N).

The positive feedback loop between the ZPA and the AER is controlled by the BMP antagonist *Grem1* (Khokha et al., 2003; Panman et al., 2006). ZPA and AER signals are prematurely lost in *Grem1* mutants causing limb patterning defects similar to those described here (Khokha et al., 2003). However, the forelimb defects cannot be attributed to loss of *Grem1* function as *Grem1* was correctly induced, albeit at lower levels, in mutant forelimb buds (Fig. 2Q,R). *Wnt7a* signalling from the dorsal ectoderm is also required for normal A-P patterning. Loss of *Wnt7a* (Parr and McMahon, 1995) or its target *Lmx1a* similarly results in loss of the ulna and posterior digits (Chen and Johnson, 2002). However, as shown in Fig. 2L, *Lmx1a* was expressed normally in the dorsal mesenchyme and histological analysis at late stages confirmed that mutant forelimbs develop normal D-V tissue polarity (see Fig. S2 in the supplementary material). Collectively, these experiments demonstrate that A-P, P-D and D-V patterning is correctly initiated at E10.5, but defects in the developing fore but not the hindlimb are caused by premature loss of the ZPA.

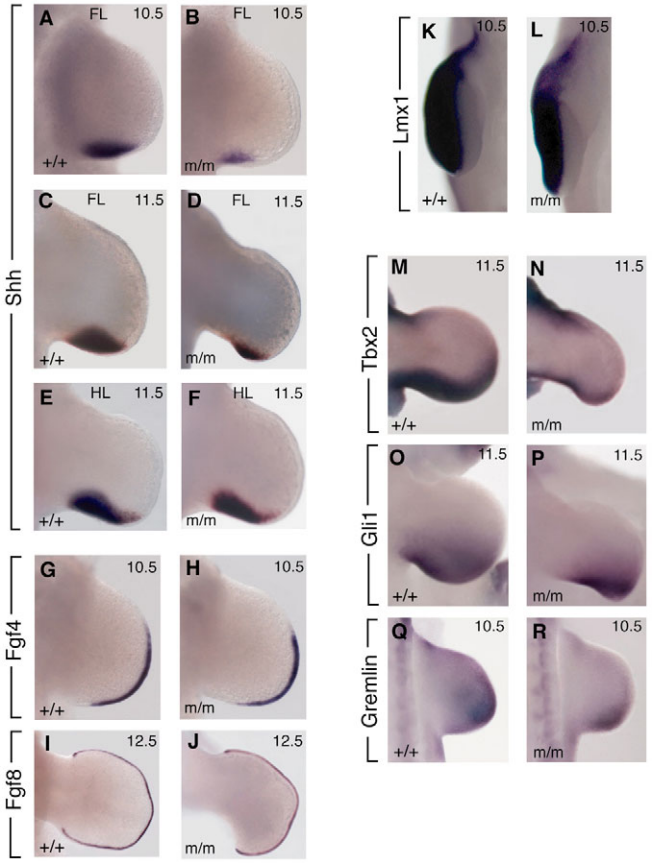

Fig. 2. *Blimp1*-deficient forelimbs fail to maintain the ZPA. Comparison of wild-type (**A**,**C**,**E**,**G**,**I**,**K**,**M**,**O**,**Q**) and mutant (**B**,**D**,**F**,**H**,**J**,**L**,**N**,**P**,**R**) forelimb (FL) and hindlimb (HL) buds. (A-C) Activation of *Shh*, a marker for the ZPA, proceeds normally at E10.5 in *Blimp*-deficient limb buds, but is markedly reduced in the forelimb bud (B). By E11.5, *Shh* expression is confined to a small patch of distal mesenchyme in mutant forelimbs (D). (H) *Blimp1* mutant limbs express *Fgf4* in the forming AER at E10.5. By contrast, by E12.5 *Fgf8* is absent from the mutant posterior proximal limb (J), owing to loss of the AER and underlying mesenchyme. *Lmx1* expression shows normal D-V patterning in the forelimb (K,L). *Tbx2* (N), and *Gli1* (P) in *Blimp1*-deficient forelimb buds highlight the rapid loss of posterior tissue. *Grem1* (Gremlin) is expressed in mutant limb buds albeit at lower levels (R).

To generate a fate map of *Blimp1*-expressing cells in the early limb bud used a *Blimp1-Cre* transgenic strain (Ohinata et al., 2005). Our results shown in Fig. 1, together with the previous work (Ohinata et al., 2005) demonstrated that *Cre* activity closely resembles the endogenous *Blimp1* expression pattern (Fig. 1I). Embryos obtained from crossing *Blimp1-Cre* males to carrying females the R26R *lacZ* reporter cassette (Soriano, 1999), were stained for β-galactosidase activity at different gestational stages. As shown in Fig. 1, Blimp1$^+$ cells gave rise to the posterior elements of the proximal limb. Blimp1$^+$ cells in the forelimb selectively formed the ulna, digits 4 and 5, and a subset of cells in digit 3 (Fig. 1J-L). Similarly in the hindlimb, Blimp1$^+$ cells represented the progenitors of the fibular and the posterior three digits (data not shown). Blimp$^+$ cells contributed to the muscles and connective tissues in the posterior fore and hindlimbs, but not the surface ectoderm (Fig. 1L). Remarkably, this fate map of Blimp1$^+$ cells could be precisely superimposed on that recently described for Shh$^+$ cells (Harfe et al., 2004). We conclude that Blimp1$^+$ Shh$^+$ progenitor

cells in the ZPA give rise to much of the proximal posterior region of the limb and this discrete cell lineage is entirely lost in *Blimp1* mutant forelimbs.

Careful histological examination, together with Lysotracker Red staining, failed to reveal any evidence for selective cell death in *Blimp1* mutant forelimbs (data not shown). Moreover staining with antibodies specific for phospho-histone3 and Ki67 at E10.5, revealed a uniform high labelling index throughout the mesenchyme in both wild-type and mutant forelimb buds (see Fig. S4 in the supplementary material).

Blimp1 is required for induction of the sensory vibrissae

By late gestation, five prominent rows of sensory vibrissae were normally visible on either side of the snout. Additionally, single or clusters of discrete whiskers were induced around the eye and on the underside of the lower jaw (Fig. 3A,C). *Blimp1* mutant embryos lacked all sensory vibrissae (Fig. 3B,D), but the other head structures that express *Blimp1*, including the papillae of the teeth and taste buds, and the neural retina (Chang et al., 2002), all developed normally (Fig. 3C,D and data not shown).

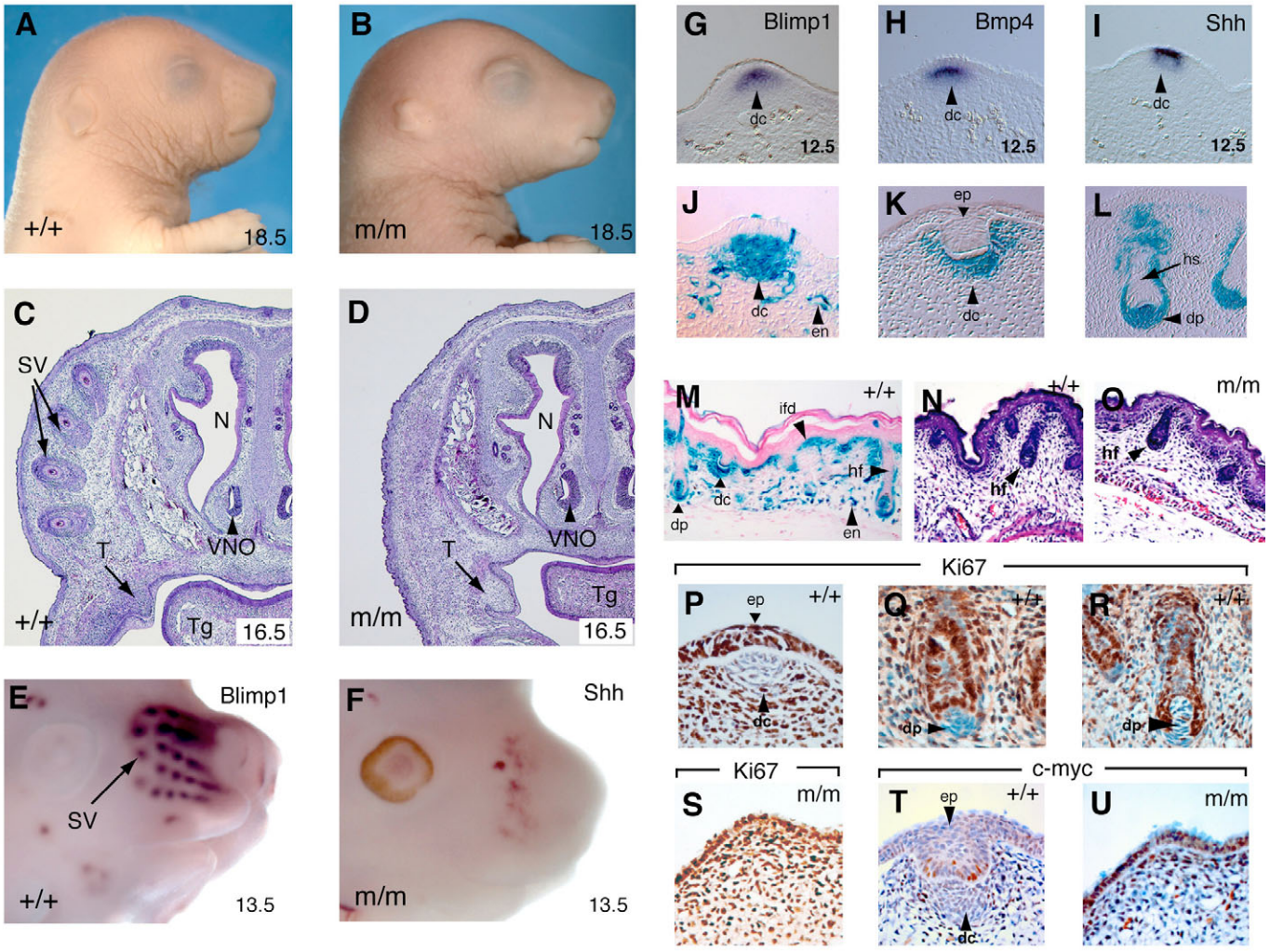

Fig. 3. *Blimp1* function in progenitors of the dermal papillae is required for induction of the sensory vibrissae. At E18.5, wild-type (**A**) embryos display five prominent rows of sensory vibrissae. These are completely absent from mutants (**B**). Frontal sections through control (**C**) and mutant (**D**) E16.5 embryos demonstrate missing vibrissae but normal tongue and tooth development. (**E**) *Blimp1* transcripts are strongly expressed in the forming vibrissae at E12.5. (**F**) *Shh* transcription is activated but not maintained in *Blimp1* mutants. (**G-I**) *Blimp1* together with *Bmp4* and *Shh* marks the mesenchymal condensates of the forming vibrissae at E12.5. Fate-mapping studies identify Blimp1$^+$ cells as giving rise to the initial condensates of the prospective dermal papilla (**J**), and underlie the invaginating ectodermal placodes (**K**), ultimately giving rise to the mature DP (**L**). Blimp1$^+$ cells that fail to incorporate into the DP migrate to surround the shaft of the forming follicle. (**M**) Fate-mapping studies show Blimp1+ cells give rise to the DP of the coat hair follicles and intrafollicular mesenchyme of the E18.5 back skin. (J,M) Punctuate *lacZ* staining marks endothelial cells. However in marked contrast to the vibrissae, histological analysis shows that hair follicle induction is *Blimp1* independent (**N**,**O**). Ki67 staining at E12.5 shows that *Blimp1* expressing cells of the dermal condensate (**P**), and DP (**Q**,**R**) are quiescent, whereas cells of the surface ectoderm, the ectodermally derived hair shaft and surrounding mesenchyme are strongly labelled. (**S**) Ki67 labelling is uniform in the mesenchyme of *Blimp1* deficient embryos. (**T**) In wild-type embryos c-myc is detected in the surrounding mesenchyme but not in the prospective DP. (**U**) c-myc-positive cells are uniformly scattered throughout both the mesenchyme and surface ectoderm in sites of vibrissae induction in *Blimp1* mutants. en, endothelial cells; dc, dermal condensates; dp, dermal papillae; hf, hair follicle; ifd, interfollicular demis; v, vibrissae; N, nares; T, teeth; Tg, tongue; VNO, vomeronasal organ.

Hair follicles are induced at two discrete stages in the developing mouse embryo. Induction of the sensory vibrissae initiates at E12.5, whereas the hair follicles of the coat, or pelage, appear several days later. Reciprocal inductive interactions between the mesenchyme of the dermis and the overlying surface ectoderm induce formation of localised thickenings or placodes that then invaginate to form the hair follicle. The underlying mesodermal cells coalesce to form the dermal papilla (reviewed by Fuchs et al., 2001; Millar, 2002; Fuchs, 2007). As shown in Fig. 3E, at E12.5 *Blimp1* localised to the mesenchymal condensates at sites of vibrissae induction, and closely overlapped with the *Bmp4* and *Shh* expression domains (Fig. 3G-I). *Blimp1* expression thus identifies the DP progenitors located under characteristic surface elevations that preconfigure the sites of ectodermal placode induction (Fig. 3G). Fate-mapping studies showed that these Blimp1$^+$ cells give rise to the mature DP and also expand to form a mesenchymal layer immediately surrounding the hair follicles (Fig. 3J-L, and data not shown). *Blimp1* expression was maintained within the mature DP (Chang et al., 2002) (data not shown) but Blimp1$^+$ progenitors not incorporated into the DP subsequently downregulated *Blimp1* expression and migrated around the sides of the hair follicle. Interestingly *Blimp1* was also expressed in the dermal condensates and prospective DP of the pelage hair follicles (Fig. 3M) but in striking contrast to sensory vibrissae, pelage hair follicles developed normally (Fig. 3N,O).

Shh, which is activated in response to Wnt/Lef1 signals from the ectoderm, is required to organise the dermal cells into focal condensates (reviewed by Fuchs, 2007). In *Blimp1* mutants *Shh*, *Bmp4* and *Gli1* expression was weakly induced, but not maintained, in the dermal mesenchyme (Fig. 3F, see Fig. S5 in the supplementary material). The surface ectoderm elevations that preconfigure the sites of vibrissae induction were visible but mutant embryos lacked localised dermal condensates and placodal thickenings (Fig. 3S). Thus *Blimp1* is required for maintenance but not initial specification of DP progenitors.

The absence of DP is not due to apoptosis of the dermal condensate because there was no evidence for foci of Lysotracker-Red-positive cells in E12.5 or 13.5 mutant embryos (data not shown). Next, we examined cell proliferation by staining with a Ki67 antibody. The prospective DP of the vibrissa was conspicuously quiescent compared with cells in the adjacent mesenchyme and overlying surface ectoderm (Fig. 3P-R). These localised foci of Ki67 negative cells were entirely absent in *Blimp1* mutant embryos. Rather the mesenchyme underlying the surface ectoderm elevations showed a uniform mitotic index (Fig. 3S).

Finally, as has been shown in B cells and the sebaceous gland (Horsley et al., 2006), we wondered whether *Blimp1* functions in DP progenitors to repress *c-myc* expression. The Ki67-negative DP cells normally failed to express c-myc (Fig. 3T) but we did not detect patches of c-myc-negative cells in the mesenchyme underneath the ectodermal elevations of *Blimp1* mutants (Fig. 3U). Rather, in *Blimp1* mutants, DP progenitors continued to divide and disperse and failed to act as localised signalling centres. Similarly, the *Shh*$^+$ cells transiently observed in E12.5 *Blimp1* mutants are also present in diffuse patches and not discrete clusters (Fig. 3F).

Functional loss of *Blimp1* disrupts pharyngeal and heart morphogenesis

The pharyngeal arches develop as a series of reiterated bulges formed in a rostral to caudal fashion. Reciprocal signalling between the surface ectoderm and endoderm, and the underlying mesoderm and neural crest (NC) cells control tissue morphogenesis. The surface epithelia expand to form discrete pouches into which the mesoderm and NC migrate (reviewed by Graham, 2001; Graham et al., 2005). We previously found that only the first arch forms and the caudal arches are completely lost in *Blimp1* null embryos (Vincent et al., 2005).

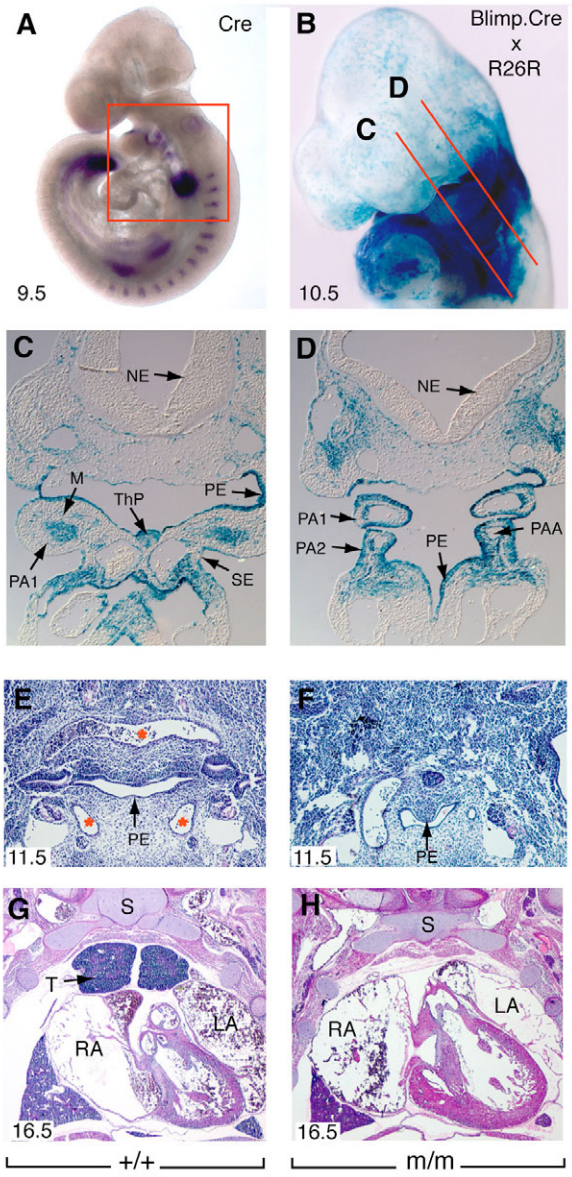

Fig. 4. *Blimp1* promotes expansion of the surface ectoderm and endoderm progenitors in the developing pharynx. (**A**) *Blimp1-Cre* faithfully recapitulates the endogenous *Blimp1* expression pattern at E9.5. (**B**) Blimp1$^+$ cells in the pharyngeal region (boxed in A) give rise to the surface epithelium of the pharyngeal arches and the anterior heart tube. (**C**,**D**) *lacZ*-marked Blimp1$^+$ cells contribute to both the surface ectoderm and pharyngeal endoderm of the pharyngeal arches, and ventral endoderm including the thyroid primordium, but are excluded from the pharyngeal mesoderm. *Blimp1* expressed in endothelial cells marks the pharyngeal arteries. (**E**,**F**) At E11.5, the *Blimp1* mutant pharynx (F) shows severe hypoplasia of the pharyngeal endoderm (PE) and pharyngeal arteries and blood vessels (asterisks) are largely absent. Frontal sections of control (**G**) and mutant (**H**) embryos show loss of the thymus in the mutants. SE, surface ectoderm; M, arch mesenchyme; NE, neurectoderm; PA pharyngeal arch; PAA, pharyngeal arch artery; PE, pharyngeal endoderm; ThP, thyroid primordium; S, sternum; T, thymus; RA, right atrium; LA left atrium.

As shown in Fig. 4, *Blimp1* was strongly expressed in the anterior epithelia of the individual pharyngeal arches (Vincent et al., 2005) (Fig. 4A). These Blimp1$^+$ cells expand rapidly giving rise to the bulk of the pharyngeal arch surface ectoderm and endoderm at E10.5 (Fig. 4B-D). Histological examination of *Sox2-Cre*-rescued *Blimp1* mutant embryos from E10.5 onwards showed that the jaws – which derive from the first pharyngeal arch – develop normally, but none of the tissue structures formed from the caudal arches are present. *Blimp1* mutants lack the thymus, which normally forms from an outpocketing of the pharyngeal endoderm of the third arch (Fig. 4G,H). Additionally, hypoplasia of the pharyngeal epithelium secondarily resulted in failure to form the pharyngeal arch arteries. The pharyngeal arch arteries normally give rise to a complex vascular network connecting the dorsal aorta to the outflow tract vessels of the heart. Loss of the pharyngeal arch artery system led to massive disturbances of the thoracic vasculature (Fig. 4E,F).

We previously found at E8.5 that *Blimp1* expression identifies a discrete sub-region of the splanchnic mesoderm (Vincent et al., 2005). By E9.5, this expression domain was positioned anteriorly and dorsal to the developing heart tube (Fig. 4A) marking the anterior or SHF progenitors of the inflow and outflow poles of the heart tube (reviewed by Buckingham et al., 2005; Srivastava, 2006). As shown in Fig. 5, Blimp1$^+$ SHF progenitors contributed almost exclusively to the myocardium of the right ventricle (RV), the ventricular septum and cells surrounding the flow tract (OFT). Relatively few marked cells were present in the left ventricle (LV) and only occasionally in the atria. At later stages (E16.5), Blimp1$^+$ descendents contributed to the walls of the aorta and pulmonary artery as well as the leaflets of the ventricular outflow valves (Fig. 5D). *Blimp1* expression thus identifies multipotent myocardial progenitor cells within the SHF (Verzi et al., 2005).

Early heart morphogenesis and formation of the right ventricle proceeded normally in *Sox2-Cre*-rescued embryos; however, at E16.5, mutant hearts (n=6) had a more pronounced apex, lacked the aortic arch and displayed persistent truncus arteriosus (PTA) and a pronounced ventricular septal defect (VSD) (Fig. 5). Thus, *Blimp1* loss disturbs alignment, septation and rotation of the arteries. *Fgf8* expression in surface epithelium, primarily the pharyngeal endoderm, promoted migration of the mesenchyme and neural crest into the forming arches. Dose-dependent *Fgf8* signalling in the SHF is required for morphogenesis of the OFT (Brown et al., 2004; Macatee et al., 2003; Park et al., 2006). Loss of the T-box transcription factor *Tbx1* also results in cardiovascular and pharyngeal defects similar to those described here (Jerome and Papaioannou, 2001; Lindsay et al., 2001; Merscher et al., 2001). *Tbx1* expression in the mesenchyme is required to support OFT morphogenesis and pharyngeal arch development, whereas expression in the endoderm is required for formation of the thymus (Zhang et al., 2006). Interestingly, at E9.5, *Fgf8* and *Tbx1* expression was severely compromised but not lost in *Blimp1*-deficient embryos (Fig. 5I-L). Thus, *Blimp1* is essential to maintain *Tbx1* and *Fgf8* expression in pharyngeal arch epithelia progenitors.

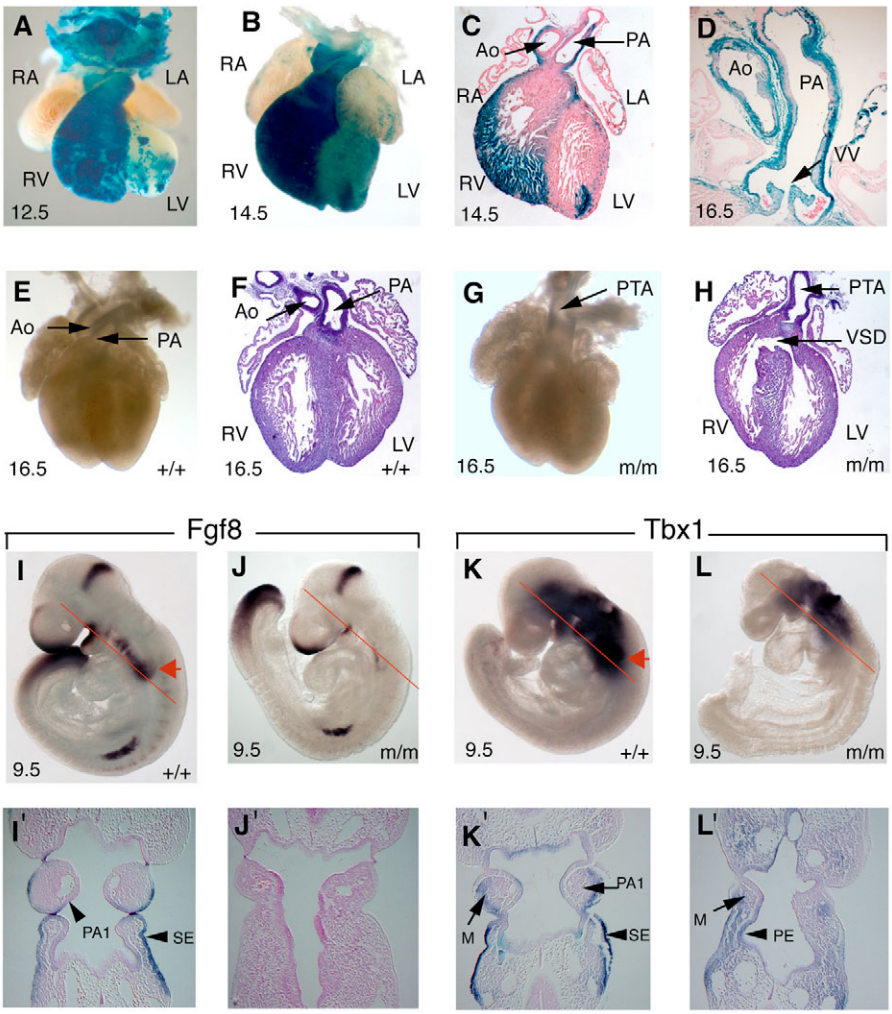

Fig. 5. Late-onset cardiac defects in *Blimp1* mutant embryos. (**A-D**) Transiently expressed *Blimp1* in the splanchnic mesoderm anterior to the heart marks progenitors of the SHF. Blimp1$^+$ cells contribute to the myocardium of the right ventricle, the outflow tract, and to the leaflets of the ventricular valves and walls of the aorta and pulmonary artery (D). (**E-H**) Outflow tract morphogenesis defects in *Blimp1*-deficient embryos (G,H) leads to persistent truncus arteriosus (PTA), in association with ventricular septal defects (VSD). *Fgf8* (**I-J'**) and *Tbx1* (**K-L'**) expression domains are severely downregulated, in part reflecting loss of the caudal pharyngeal arches (PA), and reduced staining in the surface epithelial and associated mesoderm. Red arrows indicate expression of *Fgf8* and *Tbx1* in the SHF in wild-type embryos. LV, left ventricle; RV, right ventricle; LA, left atrium; RA, right atrium; Ao, aorta; PA, pulmonary artery; VV, ventricular valves; PA, pharyngeal arch; SE, surface ectoderm; M, arch mesenchyme; PE, pharyngeal endoderm.

Table 2. Graded *Blimp1* expression levels control embryo survival

***Blimp1*$^{gfp/+}$ × *Blimp1*$^{gfp/+}$ Intercross**		
Age	Number of embryos	Recovery of *Blimp1*$^{gfp/gfp}$
E10.5	158	38 (24.0%)
E13.5	42	8 (19.0%)
E16.5	40	7 (17.5%)
***Blimp1*$^{gfp/+}$ × *Prdm1*$^{+/-}$ Intercross**		
Age	Number of embryos	Recovery of *Blimp1*$^{gfp/-}$
E13.5	30	4 (13.5%)
E14.5	17	1 (5.8%)
E15.5	18	2 (11.0%)

These results suggest that the complex pharyngeal and heart abnormalities in *Blimp1* mutant embryos are probably caused by a failure to expand and maintain signalling capabilities within the surface epithelium.

A *Blimp1*^{gfp} reporter allele reveals dose-dependent *Blimp1* functions in mouse development

A *Blimp1*^{gfp} reporter allele previously generated via insertion of a STOP-IRESgfp-pgk neo cassette 3′ to exon 6 eliminates expression of the C-terminal zinc fingers and effectively acts as a null mutation in B cells (Kallies et al., 2004). However, in contrast to the early lethality seen in *Prdm1*$^{BEH/BEH}$ and *Prdm1*$^{-/-}$ null embryos at E10.5, homozygous *Blimp1*$^{gfp/gfp}$ embryos survive to late gestational stages at almost mendelian ratios (Kallies et al., 2004) (Table 2). Because downstream coding exons remain intact, we wondered whether enhanced survival of *Blimp1*$^{gfp/gfp}$ embryos was associated with leaky expression of wild-type transcripts. To evaluate this possibility, we initially performed RT-PCR using appropriate primer combinations spanning exons 6, 7 and 8. As shown in Fig. 6A, in addition to transcripts that prematurely terminate within the IRESgfp-pgk neo cassette, *Blimp1*$^{gfp/gfp}$ embryos expressed correctly spliced wild-type transcripts. Similar conclusions were reached in RPA experiments (data not shown).

Western blot experiments demonstrate that LPS-activated heterozygous *Blimp1*$^{gfp/+}$ spleen cells and *Blimp1*$^{gfp/gfp}$ embryos produce truncated Blimp1 protein lacking the C-terminal zinc-finger domains (Kallies et al., 2004). However, we also clearly detect full-length Blimp1 protein in E9.5 *Blimp1*$^{gfp/gfp}$ embryos (Fig. 6B). We also engineered an expression vector via introduction of a stop codon at amino acid 556. In contrast to full-length Blimp1, truncated Blimp1 protein lacking the zinc fingers failed to enter the nucleus (Fig. 6C). Collectively, these results strongly suggest that the truncated Blimp1 protein encoded by the gfp reporter allele has no functional activity. Rather the enhanced survival of *Blimp1*$^{gfp/gfp}$ embryos can best be explained by low levels of full-length mRNA and protein expression.

Interestingly, *Blimp1*$^{gfp/gfp}$ mutant embryos (n=5) displayed the identical pharyngeal and cardiovascular defects as described above for *Blimp1* mutant embryos, including PTA and VSD (Fig. 7A,B). However, forelimb development was less severely compromised. In most cases the ulna formed correctly and only a single posterior digit was absent (Fig. 7G). Moreover, induction of the sensory vibrissae occurred normally (Fig. 7J). Interestingly reduced numbers of PGCs were detectable in heterozygous *Blimp1*$^{gfp/+}$ littermates whereas none of 12 E9.5 *Blimp1*$^{gfp/gfp}$ embryos contained alkaline-

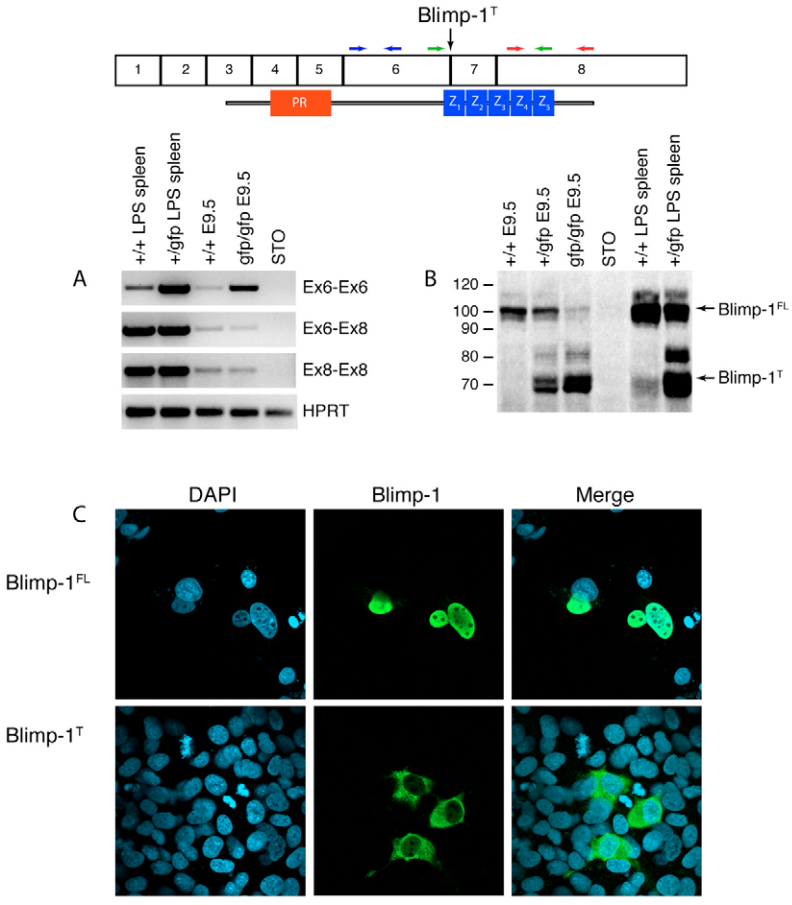

Fig. 6. Molecular characterisation of the *Blimp1*^{gfp} locus. (Top) An IRES-gfp reporter cassette inserted 3′ to exon 6 predominantly leads to expression of truncated Blimp1 protein (Blimp-1^{T}) lacking the C-terminal zinc fingers (Z1-Z5) owing to the presence of inframe stop codons. Arrows indicate position of PCR primers used to amplify exon 6 (blue), exon 6-8 (green) and exon 8 (red) sequences. (**A**) RT-PCR analysis reveals correctly spliced transcripts containing exons 6,7 and 8. (**B**) Western blot experiments also demonstrate wild-type protein expression in homozygous *Blimp1*$^{gfp/gfp}$ embryos. These results are representative of three independent experiments analysing individually genotyped wild-type (n=8), *gfp/+* (n=8) and *gfp/gfp* (n=7) embryos. Molecular size markers in KDa are on the left. (**C**) COS cells transiently transfected with expression constructs encoding full-length (FL) or truncated (T) Blimp1 protein, were stained with monoclonal anti-Blimp1 antibody and analysed by confocal microscopy. In striking contrast to the wild-type protein, truncated Blimp1 lacking the C-terminal zinc fingers fails to enter the nucleus.

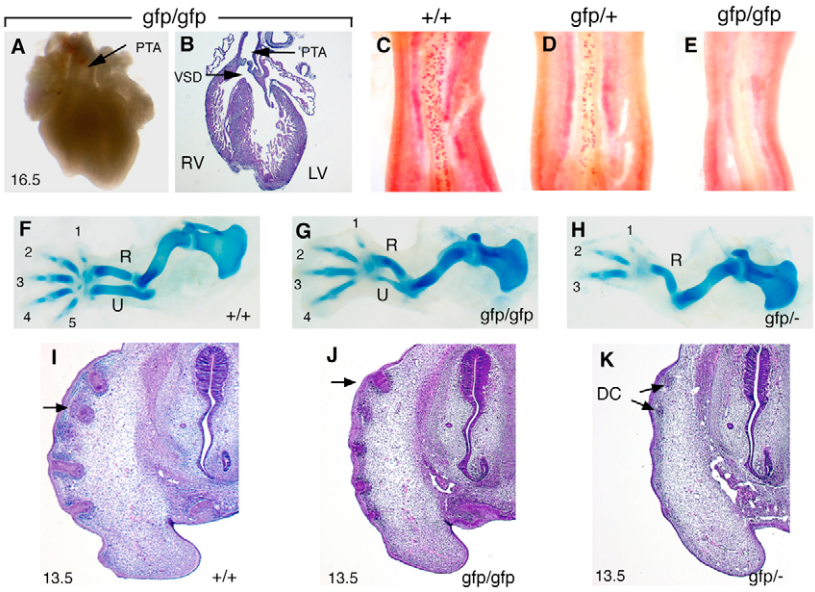

Fig. 7. Graded *Blimp1* activities required for germ cell specification and development of the cardiovascular system, forelimbs and vibrissae. (**A**,**B**) Homozygous *Blimp1*$^{gfp/gfp}$ embryos display cardiovascular defects including PTA and VSD. Fast Red alkaline phosphatase staining of PGCs in the dorsal hindgut of wild-type (**C**), *gfp*/+ (**D**) and *gfp/gfp* (**E**) E9.5 embryos. Decreased numbers of PGCs are specified in *gfp*/+ embryos and homozygous mutants entirely lack PGCs. (**F-H**) Homozygous *gfp/gfp* forelimbs contain a rudimentary ulna and four digits (G). Heterozygous *gfp*/– embryos with further reduced *Blimp1* activity entirely lack the ulna and are missing the posterior two digits. (**I**,**J**) Induction of the sensory vibrissae is relatively *Blimp1* independent because vibrissae induction is unperturbed (arrows), and ectodermal placode induction and invagination occurs normally in *gfp/gfp* homozygous embryos (J). *Blimp1* expression in *gfp*/– embryos is sufficient for coalescence of the prospective DP cells, but these fail to induce overlying ectodermal placodes (**K**). DC, dermal condensates; LV, left ventricle; PTA, persistent truncus arteriosus; R, radius; RV, right ventricle; U, ulna; VSD, ventricular septal defect.

phosphatase-positive PGCs (Fig. 7C,D). Homozygous *Blimp1*$^{gfp/gfp}$ embryos thus completely lacked germ cells and in this respect phenocopy the null mutants (Fig. 7E).

Next, to examine the consequences of further reduced *Blimp1* expression levels heterozygotes carrying the hypomorphic *Blimp1*$^{gfp/+}$ allele and the *Blimp1*$^{BEH/+}$ null allele (Vincent et al., 2005) were intercrossed to generate transheterozygous *Blimp1*$^{gfp/–}$ embryos. Only a small proportion survive to E13.5 (Table 2). As for *Blimp1* mutant embryos, both the ulna and posterior digits were missing (Fig. 7H), and interestingly the dermal condensates of the vibrissae were induced to form; however, only a small fraction of these proceeded to the ectodermal placode stage (Fig. 7K). We conclude that weak *Blimp1* expression is sufficient to promote development of the extra-embryonic tissues, sensory vibrissae and the posterior forelimb, whereas increased *Blimp1* activities are required for pharyngeal and heart morphogenesis, and PGC specification requires highest levels of *Blimp1* expression.

DISCUSSION

Blimp1 null embryos arrest at around E9.5-10.5 because of an underdeveloped labyrinth: the region of the placenta responsible for maternal foetal exchange (Vincent et al., 2005). Bypassing *Blimp1* requirements in extra-embryonic tissues allowed us to rescue the early lethality and demonstrate essential roles in the posterior forelimb, caudal pharyngeal arches, OFT of the heart, and dermal papillae of the sensory whiskers. *Blimp1* expression identifies multipotent progenitor cell populations allocated during tissue morphogenesis and is essential for maintenance of key signalling centres guiding cell proliferation and differentiation within these complex structures.

Blimp1 functional loss disrupts development of the highly specialised sensory vibrissae. *Blimp1* expression in the dermal condensates marks islands of quiescent cells within the expanding population of head mesenchyme. *Blimp1* induced in response to instructive signals from the surface ectoderm, represses c-myc expression, arrests cell division, and causes cells to coalesce and form a signalling centre. Neighbouring cells continue to rapidly divide and disperse into the surrounding mesenchyme.

Time-dependent Shh signalling in the ZPA controls specification of the tissues of the posterior limb (reviewed by Tickle, 2006). Likewise, *Blimp1* is required in multipotent progenitors giving rise to the skeletal elements, muscles and connective tissue of the posterior forelimb. Our results demonstrate that *Blimp1* maintains this short-lived progenitor cell population. However, *Blimp1* is not essential for *Shh* activation because the onset of *Blimp1* expression in the prospective ZPA of the forelimb occurs around day 9 of development, well in advance of *Shh*. Moreover, early forelimb patterning proceeds normally in *Blimp1* mutant embryos.

Similarly fate-mapping experiments show that transient *Blimp1* expression in the forming pharyngeal arches is essential for expansion of ectodermal and endodermal progenitors giving rise to the entire surface epithelia of the pharynx. Loss of *Blimp1* function results in downregulated *Tbx1* and *Fgf8* expression in the surface epithelia leading to selective loss of the mesenchyme and NC that normally migrate into the caudal pharyngeal arches. The failure to elaborate the caudal pharyngeal arches disrupts development of the PA arteries. NC that invade the OFT are required for separation of the arteries and formation of the outflow valves (reviewed by Jiang et al., 2000). Abnormal morphogenesis of the OFT and ventricular septum could thus potentially reflect hypoplasia of the pharyngeal epithelia and concomitant loss of invading NC that normally migrate through the caudal pharyngeal arches and surround the outflow region (Jiang et al., 2000). *Shh* expression in the ventral pharyngeal endoderm is known to be required for OFT morphogenesis (Goddeeris et al., 2007), partly because of its ability to promote NC survival. However, loss of *Shh* in the ventral endoderm fails to disrupt pharyngeal arch development, and *Fgf8* and *Tbx1* expression is unperturbed (Goddeeris et al., 2007). PTA has also been observed in Pitx2δc mutants in a context where NC migration occurs normally (Liu et al., 2002). To clarify the underlying cause of these OFT and PTA defects, future studies aim to selectively inactivate *Blimp1* in either the pharyngeal epithelia or the SHF.

This cluster of pharyngeal and heart defects closely resembles those associated with DiGeorge syndrome (DGS), highly prevalent in the human population (reviewed by Lindsay, 2001). In mice, *Tbx1* haploinsufficiency causes aortic arch defects (Jerome and Papaioannou, 2001; Lindsay et al., 2001; Merscher et al., 2001), and *Tbx1* maps to the DGS interval del22q11 in humans. Manipulating Fgf8 and Tbx1 expression also leads to DGS phenotypes in mice (Brown et al., 2004; Macatee et al., 2003; Park et al., 2006; Zhang

et al., 2006). It will be interesting to learn whether *Blimp1* mutations are causally associated with DGS and congenital heart defects in the human population.

In zebrafish *Blimp1* (also known as *prdm1* – ZFIN) is expressed in the mesenchyme as well as the ectodermal cells of the early fin bud and later in the cells of the AER. In *ubo* mutants, loss of *Blimp1* activity severely impairs pectoral fin outgrowth and patterning (Lee and Roy, 2006), whereas *Blimp1* morphant embryos entirely lack fin buds (Mercader et al., 2006). *Blimp1* acts downstream of *Shh* signalling for specification of the slow-twitch muscle lineage (Baxendale et al., 2004), and in the neural crest, *Blimp1* functions downstream of *Bmp* signalling to promote formation of sensory neuron progenitors (Hernandez-Lagunas et al., 2005; Roy and Ng, 2004). However, experiments to date strongly suggest that *Blimp1* is not required in either muscle or neural crest lineages in mice. In light of these differences, we conclude that Blimp1 functions in the fin and limb are not conserved between fish and mammals.

Blimp1 is essential for specification of primordial germ cells (Ohinata et al., 2005; Surani et al., 2007). In the developing mouse embryo, *Blimp1* induced in the proximal epiblast in response to BMP/Smad signals (Lawson et al., 1999; Tremblay et al., 2001; Chu et al., 2004; Arnold et al., 2006) represses the default pathway that would normally give rise to posterior mesodermal derivatives such as the allantois or the primitive streak. However, *Blimp1* contributions to the germ cell lineage appear to be mammalian specific because *Blimp1* is not expressed in zebrafish PGCs (Ng et al., 2006). Similarly, the present experiments establish that *Blimp1* is required in trophoblast cells of the labyrinthine placenta, a uniquely mammalian cell lineage. Collectively these observations strongly suggest that diverse tissue-specific transcriptional networks controlled by *Blimp1* as a master regulator have evolved independently in different organisms.

The tumour suppressor p53 regulates the expression of numerous target genes to protect cells against genotoxic stress. Recent studies have identified *Blimp1* as a p53 target (Yan et al., 2007). The NC and mesenchyme of the prospective caudal arches in *Blimp1* null embryos undergoes apoptosis (Vincent et al., 2005). However, the dying cells are not Blimp1$^+$ and cell death most likely occurs as a secondary consequence of loss of *Fgf8* expression in the pharyngeal epithelia (Macatee et al., 2003). Moreover, we found no evidence that apoptosis contributes to any of the tissue abnormalities described here. Interestingly, *p63* is strongly expressed in embryonic epithelia at sites undergoing reciprocal signalling. Strikingly, as for *Blimp1* mutants, *p63*-deficient embryos display limb defects, pharyngeal arch hypoplasia, and lack epithelial structures including the vibrissae and hair (Mills et al., 1999; Yang et al., 1999). It will be interesting to learn whether *p63* and *Blimp1* cooperatively govern self-renewal of diverse progenitor cell populations in the pharyngeal surface epithelium.

Blimp1 selectively maintains the ZPA in the forelimb but not the hindlimb. Similarly, *Blimp1* is required for induction of sensory vibrissae but not pelage hair follicles. One possibility is that yet-to-be-discovered, divergent signalling pathways may selectively control development of these morphologically similar structures. Alternatively, closely related zinc-finger PR/SET domain family members may selectively compensate for the loss of *Blimp1* activity in the developing hindlimb and pelage hair follicles. More than 15 PRDM genes have been identified and several have been shown to control embryonic development (Hoyt et al., 1997) and/or tumour growth (Steele-Perkins et al., 2001). An important future goal is to test whether additional members of the PRDM family are coexpressed with *Blimp1* in these unaffected tissues.

The present experiments demonstrate that homozygous *Blimp1*$^{gfp/gfp}$ embryos carrying an IRESgfp reporter cassette, only weakly express *Blimp1* but entirely lack PGCs and display fully penetrant pharyngeal and heart defects, whereas extra-embryonic tissues and sensory vibrissae develop normally. More pronounced defects were observed in transheterozygous *Blimp1*$^{gfp/-}$ embryos, with further reduced expression levels. These results demonstrate graded *Blimp1* activities in the developing mouse embryo and strongly suggest that moderate changes in *Blimp1* expression levels may have a significant impact on target gene selection and/or *Blimp1* functions as a scaffolding protein for recruitment of co-repressors.

We thank Kathryn Calame for the *Blimp1* conditional mice, Azim Surani and Michel Nussenzweig for the *Blimp1-Cre* mice, Lynn Corcoran for Blimp1 antibody, John Fallon, Malcolm Logan, Peter Scambler and Rolf Zeller for probes, and Andreas Trumpp and Albert Basson for c-myc and Lysotracker Red staining protocols, respectively. This work was supported by a programme grant from the Wellcome Trust.

Supplementary material

Supplementary material for this article is available at http://dev.biologists.org/cgi/content/full/134/24/4335/DC1

References

Ancelin, K., Lange, U. C., Hajkova, P., Schneider, R., Bannister, A. J., Kouzarides, T. and Surani, M. A. (2006). Blimp1 associates with Prmt5 and directs histone arginine methylation in mouse germ cells. *Nat. Cell Biol.* **8**, 623-630.

Arnold, S. J., Maretto, S., Islam, A., Bikoff, E. K. and Robertson, E. J. (2006). Dose-dependent Smad1, Smad5 and Smad8 signaling in the early mouse embryo. *Dev. Biol.* **296**, 104-118.

Baxendale, S., Davison, C., Muxworthy, C., Wolff, C., Ingham, P. W. and Roy, S. (2004). The B-cell maturation factor Blimp-1 specifies vertebrate slow-twitch muscle fiber identity in response to Hedgehog signaling. *Nat. Genet.* **36**, 88-93.

Brown, C. B., Wenning, J. M., Lu, M. M., Epstein, D. J., Meyers, E. N. and Epstein, J. A. (2004). Cre-mediated excision of Fgf8 in the Tbx1 expression domain reveals a critical role for Fgf8 in cardiovascular development in the mouse. *Dev. Biol.* **267**, 190-202.

Buckingham, M., Meilhac, S. and Zaffran, S. (2005). Building the mammalian heart from two sources of myocardial cells. *Nat. Rev. Genet.* **6**, 826-835.

Chang, D. H., Cattoretti, G. and Calame, K. L. (2002). The dynamic expression pattern of B lymphocyte induced maturation protein-1 (Blimp-1) during mouse embryonic development. *Mech. Dev.* **117**, 305-309.

Chen, H. and Johnson, R. L. (2002). Interactions between dorsal-ventral patterning genes lmx1b, engrailed-1 and wnt-7a in the vertebrate limb. *Int. J. Dev. Biol.* **46**, 937-941.

Chu, G. C., Dunn, N. R., Anderson, D. C., Oxburgh, L. and Robertson, E. J. (2004). Differential requirements for Smad4 in TGFbeta-dependent patterning of the early mouse embryo. *Development* **131**, 3501-3512.

Fuchs, E. (2007). Scratching the surface of skin development. *Nature* **445**, 834-842.

Fuchs, E., Merrill, B. J., Jamora, C. and DasGupta, R. (2001). At the roots of a never-ending cycle. *Dev. Cell* **1**, 13-25.

Goddeeris, M. M., Schwartz, R., Klingensmith, J. and Meyers, E. N. (2007). Independent requirements for Hedgehog signaling by both the anterior heart field and neural crest cells for outflow tract development. *Development* **134**, 1593-1604.

Gong, D. and Malek, T. R. (2007). Cytokine-dependent Blimp-1 expression in activated T cells inhibits IL-2 production. *J. Immunol.* **178**, 242-252.

Graham, A. (2001). The development and evolution of the pharyngeal arches. *J. Anat.* **199**, 133-141.

Graham, A., Okabe, M. and Quinlan, R. (2005). The role of the endoderm in the development and evolution of the pharyngeal arches. *J. Anat.* **207**, 479-487.

Gyory, I., Fejer, G., Ghosh, N., Seto, E. and Wright, K. L. (2003). Identification of a functionally impaired positive regulatory domain I binding factor 1 transcription repressor in myeloma cell lines. *J. Immunol.* **170**, 3125-3133.

Gyory, I., Wu, J., Fejer, G., Seto, E. and Wright, K. L. (2004). PRDI-BF1 recruits the histone H3 methyltransferase G9a in transcriptional silencing. *Nat. Immunol.* **5**, 299-308.

Harfe, B. D., Scherz, P. J., Nissim, S., Tian, H., McMahon, A. P. and Tabin, C. J. (2004). Evidence for an expansion-based temporal Shh gradient in specifying vertebrate digit identities. *Cell* **118**, 517-528.

Hayashi, K., de Sousa Lopes, S. M. and Surani, M. A. (2007). Germ cell specification in mice. *Science* **316**, 394-396.

Hayashi, S., Lewis, P., Pevny, L. and McMahon, A. P. (2002). Efficient gene

modulation in mouse epiblast using a Sox2Cre transgenic mouse strain. *Gene Expr. Patterns* **2**, 93-97.
Hernandez-Lagunas, L., Choi, I. F., Kaji, T., Simpson, P., Hershey, C., Zhou, Y., Zon, L., Mercola, M. and Artinger, K. B. (2005). Zebrafish narrowminded disrupts the transcription factor prdm1 and is required for neural crest and sensory neuron specification. *Dev. Biol.* **278**, 347-357.
Horsley, V., O'Carroll, D., Tooze, R., Ohinata, Y., Saitou, M., Obukhanych, T., Nussenzweig, M., Tarakhovsky, A. and Fuchs, E. (2006). Blimp1 defines a progenitor population that governs cellular input to the sebaceous gland. *Cell* **126**, 597-609.
Hoyt, P. R., Bartholomew, C., Davis, A. J., Yutzey, K., Gamer, L. W., Potter, S. S., Ihle, J. N. and Mucenski, M. L. (1997). The Evi1 proto-oncogene is required at midgestation for neural, heart, and paraxial mesenchyme development. *Mech. Dev.* **65**, 55-70.
Jerome, L. A. and Papaioannou, V. E. (2001). DiGeorge syndrome phenotype in mice mutant for the T-box gene, Tbx1. *Nat. Genet.* **27**, 286-291.
Jiang, X., Rowitch, D. H., Soriano, P., McMahon, A. P. and Sucov, H. M. (2000). Fate of the mammalian cardiac neural crest. *Development* **127**, 1607-1616.
Kallies, A. and Nutt, S. L. (2007). Terminal differentiation of lymphocytes depends on Blimp-1. *Curr. Opin. Immunol.* **19**, 156-162.
Kallies, A., Hasbold, J., Tarlinton, D. M., Dietrich, W., Corcoran, L. M., Hodgkin, P. D. and Nutt, S. L. (2004). Plasma cell ontogeny defined by quantitative changes in blimp-1 expression. *J. Exp. Med.* **200**, 967-977.
Kallies, A., Hawkins, E. D., Belz, G. T., Metcalf, D., Hommel, M., Corcoran, L. M., Hodgkin, P. D. and Nutt, S. L. (2006). Transcriptional repressor Blimp-1 is essential for T cell homeostasis and self-tolerance. *Nat. Immunol.* **7**, 466-474.
Keller, A. D. and Maniatis, T. (1991). Identification and characterization of a novel repressor of beta-interferon gene expression. *Genes Dev.* **5**, 868-879.
Keller, A. D. and Maniatis, T. (1992). Only two of the five zinc fingers of the eukaryotic transcriptional repressor PRDI-BF1 are required for sequence-specific DNA binding. *Mol. Cell. Biol.* **12**, 1940-1949.
Khokha, M. K., Hsu, D., Brunet, L. J., Dionne, M. S. and Harland, R. M. (2003). Gremlin is the BMP antagonist required for maintenance of Shh and Fgf signals during limb patterning. *Nat. Genet.* **34**, 303-307.
Kisanuki, Y. Y., Hammer, R. E., Miyazaki, J., Williams, S. C., Richardson, J. A. and Yanagisawa, M. (2001). Tie2-Cre transgenic mice: a new model for endothelial cell-lineage analysis in vivo. *Dev. Biol.* **230**, 230-242.
Lawson, K. A., Dunn, N. R., Roelen, B. A., Zeinstra, L. M., Davis, A. M., Wright, C. V., Korving, J. P. and Hogan, B. L. (1999). Bmp4 is required for the generation of primordial germ cells in the mouse embryo. *Genes Dev.* **13**, 424-436.
Lee, B. C. and Roy, S. (2006). Blimp-1 is an essential component of the genetic program controlling development of the pectoral limb bud. *Dev. Biol.* **300**, 623-634.
Lin, Y., Wong, K. and Calame, K. (1997). Repression of c-myc transcription by Blimp-1, an inducer of terminal B cell differentiation. *Science* **276**, 596-599.
Lindsay, E. A. (2001). Chromosomal microdeletions: dissecting del22q11 syndrome. *Nat. Rev. Genet.* **2**, 858-868.
Lindsay, E. A., Vitelli, F., Su, H., Morishima, M., Huynh, T., Pramparo, T., Jurecic, V., Ogunrinu, G., Sutherland, H. F., Scambler, P. J. et al. (2001). Tbx1 haploinsufficieny in the DiGeorge syndrome region causes aortic arch defects in mice. *Nature* **410**, 97-101.
Liu, C., Liu, W., Palie, J., Lu, M. F., Brown, N. A. and Martin, J. F. (2002). Pitx2c patterns anterior myocardium and aortic arch vessels and is required for local cell movement into atrioventricular cushions. *Development* **129**, 5081-5091.
Macatee, T. L., Hammond, B. P., Arenkiel, B. R., Francis, L., Frank, D. U. and Moon, A. M. (2003). Ablation of specific expression domains reveals discrete functions of ectoderm- and endoderm-derived FGF8 during cardiovascular and pharyngeal development. *Development* **130**, 6361-6374.
Martins, G. A., Cimmino, L., Shapiro-Shelef, M., Szabolcs, M., Herron, A., Magnusdottir, E. and Calame, K. (2006). Transcriptional repressor Blimp-1 regulates T cell homeostasis and function. *Nat. Immunol.* **7**, 457-465.
McGlinn, E. and Tabin, C. J. (2006). Mechanistic insight into how Shh patterns the vertebrate limb. *Curr. Opin. Genet. Dev.* **16**, 426-432.
Mercader, N., Fischer, S. and Neumann, C. J. (2006). Prdm1 acts downstream of a sequential RA, Wnt and Fgf signaling cascade during zebrafish forelimb induction. *Development* **133**, 2805-2815.
Merscher, S., Funke, B., Epstein, J. A., Heyer, J., Puech, A., Lu, M. M., Xavier, R. J., Demay, M. B., Russell, R. G., Factor, S. et al. (2001). TBX1 is responsible for cardiovascular defects in velo-cardio-facial/DiGeorge syndrome. *Cell* **104**, 619-629.
Millar, S. E. (2002). Molecular mechanisms regulating hair follicle development. *J. Invest. Dermatol.* **118**, 216-225.
Mills, A. A., Zheng, B., Wang, X. J., Vogel, H., Roop, D. R. and Bradley, A. (1999). p63 is a p53 homologue required for limb and epidermal morphogenesis. *Nature* **398**, 708-713.
Nagy, A., Gertsenstein, M., Vintersten, K. and Behringer, R. (2003). *Manipulating the Mouse Embryo: A Laboratory Manual* (3rd edn). Cold Spring Harbor, NY: Cold Spring Harbor Laboratory Press.
Ng, T., Yu, F. and Roy, S. (2006). A homologue of the vertebrate SET domain and zinc finger protein Blimp-1 regulates terminal differentiation of the tracheal system in the Drosophila embryo. *Dev. Genes Evol.* **216**, 243-252.
Niwa, H., Yamamura, K. and Miyazaki, J. (1991). Efficient selection for high-expression transfectants with a novel eukaryotic vector. *Gene* **108**, 193-199.
Ohinata, Y., Payer, B., O'Carroll, D., Ancelin, K., Ono, Y., Sano, M., Barton, S. C., Obukhanych, T., Nussenzweig, M., Tarakhovsky, A. et al. (2005). Blimp1 is a critical determinant of the germ cell lineage in mice. *Nature* **436**, 207-213.
Panman, L., Galli, A., Lagarde, N., Michos, O., Soete, G., Zuniga, A. and Zeller, R. (2006). Differential regulation of gene expression in the digit forming area of the mouse limb bud by SHH and gremlin 1/FGF-mediated epithelial-mesenchymal signalling. *Development* **133**, 3419-3428.
Park, E. J., Ogden, L. A., Talbot, A., Evans, S., Cai, C. L., Black, B. L., Frank, D. U. and Moon, A. M. (2006). Required, tissue-specific roles for Fgf8 in outflow tract formation and remodeling. *Development* **133**, 2419-2433.
Parr, B. A. and McMahon, A. P. (1995). Dorsalizing signal Wnt-7a required for normal polarity of D-V and A-P axes of mouse limb. *Nature* **374**, 350-353.
Ren, B., Chee, K. J., Kim, T. H. and Maniatis, T. (1999). PRDI-BF1/Blimp-1 repression is mediated by corepressors of the Groucho family of proteins. *Genes Dev.* **13**, 125-137.
Roy, S. and Ng, T. (2004). Blimp-1 specifies neural crest and sensory neuron progenitors in the zebrafish embryo. *Curr. Biol.* **14**, 1772-1777.
Shaffer, A. L., Lin, K. I., Kuo, T. C., Yu, X., Hurt, E. M., Rosenwald, A., Giltnane, J. M., Yang, L., Zhao, H., Calame, K. et al. (2002). Blimp-1 orchestrates plasma cell differentiation by extinguishing the mature B cell gene expression program. *Immunity* **17**, 51-62.
Shaffer, A. L., Shapiro-Shelef, M., Iwakoshi, N. N., Lee, A. H., Qian, S. B., Zhao, H., Yu, X., Yang, L., Tan, B. K., Rosenwald, A. et al. (2004). XBP1, downstream of Blimp-1, expands the secretory apparatus and other organelles, and increases protein synthesis in plasma cell differentiation. *Immunity* **21**, 81-93.
Shapiro-Shelef, M. and Calame, K. (2005). Regulation of plasma-cell development. *Nat. Rev. Immunol.* **5**, 230-242.
Shapiro-Shelef, M., Lin, K. I., McHeyzer-Williams, L. J., Liao, J., McHeyzer-Williams, M. G. and Calame, K. (2003). Blimp-1 is required for the formation of immunoglobulin secreting plasma cells and pre-plasma memory B cells. *Immunity* **19**, 607-620.
Soriano, P. (1999). Generalized lacZ expression with the ROSA26 Cre reporter strain. *Nat. Genet.* **21**, 70-71.
Srivastava, D. (2006). Making or breaking the heart: from lineage determination to morphogenesis. *Cell* **126**, 1037-1048.
Steele-Perkins, G., Fang, W., Yang, X. H., Van Gele, M., Carling, T., Gu, J., Buyse, I. M., Fletcher, J. A., Liu, J., Bronson, R. et al. (2001). Tumor formation and inactivation of RIZ1, an Rb-binding member of a nuclear protein-methyltransferase superfamily. *Genes Dev.* **15**, 2250-2262.
Surani, M. A., Hayashi, K. and Hajkova, P. (2007). Genetic and epigenetic regulators of pluripotency. *Cell* **128**, 747-762.
Tickle, C. (2006). Making digit patterns in the vertebrate limb. *Nat. Rev. Mol. Cell Biol.* **7**, 45-53.
Tremblay, K. D., Dunn, N. R. and Robertson, E. J. (2001). Mouse embryos lacking Smad1 signals display defects in extra-embryonic tissues and germ cell formation. *Development* **128**, 3609-3621.
Tunyaplin, C., Shapiro, M. A. and Calame, K. L. (2000). Characterization of the B lymphocyte-induced maturation protein-1 (Blimp-1) gene, mRNA isoforms and basal promoter. *Nucleic Acids Res.* **28**, 4846-4855.
Turner, C. A., Jr, Mack, D. H. and Davis, M. M. (1994). Blimp-1, a novel zinc finger-containing protein that can drive the maturation of B lymphocytes into immunoglobulin-secreting cells. *Cell* **77**, 297-306.
Verzi, M. P., McCulley, D. J., De Val, S., Dodou, E. and Black, B. L. (2005). The right ventricle, outflow tract, and ventricular septum comprise a restricted expression domain within the secondary/anterior heart field. *Dev. Biol.* **287**, 134-145.
Vincent, S. D., Dunn, N. R., Sciammas, R., Shapiro-Shalef, M., Davis, M. M., Calame, K., Bikoff, E. K. and Robertson, E. J. (2005). The zinc finger transcriptional repressor Blimp1/Prdm1 is dispensable for early axis formation but is required for specification of primordial germ cells in the mouse. *Development* **132**, 1315-1325.
Yan, J., Jiang, J., Lim, C. A., Wu, Q., Ng, H. H. and Chin, K. C. (2007). BLIMP1 regulates cell growth through repression of p53 transcription. *Proc. Natl. Acad. Sci. USA* **104**, 1841-1846.
Yang, A., Schweitzer, R., Sun, D., Kaghad, M., Walker, N., Bronson, R. T., Tabin, C., Sharpe, A., Caput, D., Crum, C. et al. (1999). p63 is essential for regenerative proliferation in limb, craniofacial and epithelial development. *Nature* **398**, 714-718.
Yu, J., Angelin-Duclos, C., Greenwood, J., Liao, J. and Calame, K. (2000). Transcriptional repression by blimp-1 (PRDI-BF1) involves recruitment of histone deacetylase. *Mol. Cell. Biol.* **20**, 2592-2603.
Zhang, Z., Huynh, T. and Baldini, A. (2006). Mesodermal expression of Tbx1 is necessary and sufficient for pharyngeal arch and cardiac outflow tract development. *Development* **133**, 3587-3595.